A simplified vector-based method for irradiance prediction at urban scale

Wei Liao, Yeonsook Heo
University of Cambridge, Cambridge, United Kingdom

Abstract

This paper presents a simplified vector-based method for predicting irradiance in urban context by taking a different approach for sky discretisation, obstruction detection and reflection models. A case study with three urban areas with varying densities is performed to validate the proposed model against the advanced simulation software, RADIANCE.

Introduction

Owing to improved solar technologies and increasing acceptance by the public, solar energy utilisation is considered as one of the most promising ways to provide renewable energy to buildings. Beyond standard PV panels, different solar technologies including Building Integrated Photovoltaic (BIPV), solar thermal collector (STC) and other solar design strategies have been increasingly adopted by city planners and architects as a way to provide energy supply in urban environment. For design and implementation of solar technologies in urban areas, it is important to assess the solar availability (Compagnon, 2004) with consideration of existing urban context or new urban developments. Solar availability is usually presented as the amount of solar irradiance by surface area during a targeting period (e.g., peak hours, daily, monthly, or yearly). Prediction of solar irradiance has been performed to evaluate possible consequences of planning policies and guidelines on solar availability (Kanters and Wall, 2016) and quantify the impact of new urban developments on existing solar collectors (Zomer and Rüther, 2017). Prediction of solar irradiance is also a necessary step to identify the most solar-potential locations in the urban fabric for solar collectors.

Unlike solar farms in rural areas, evaluating solar irradiance in cities is a difficult problem as urban areas are densely filled with many buildings that create mutual shading and reflection. A range of different approaches have been investigated in the past decade to predict solar irradiance at urban scale. Existing approaches can be categorised broadly into two groups: raster-based approaches and vector-based approaches.

Raster-based approaches create Digital Surface Model (DSM) on the basis of existing GIS data, which represents the urban fabric, including terrain, building footprints and heights, as a 2.5D raster grid. ArcGis Solar Analyst (Fu and Rich, 2002) and the GRASS r.sun (Hofierka and Suri, 2002) are 2.5D raster-based calculation methods that mainly consider terrain elevation without consideration of buildings for predicting solar irradiance on horizontal surface at continental or regional scale (Hofierka and Kanuk, 2009). Instead of using traditional GIS data, Technology of Light Detection And Ranging (LiDAR) was developed to detect objects in urban areas and identify them into vegetation, ground, building façades with footprints and heights. High-resolution urban data from LiDAR allows for creating DSMs that represent the actual urban context with better details. With improved raster-based DSMs, researchers (Redweik, et al., 2013;Lindberg, et al., 2015) have developed different shadow calculation models to determine daylight obstruction for predicting irradiance on building roofs and facades. Redweik, et al. (2013) developed a shadow model by introducing hyperpoints for each pixel (i.e., several Z values in the same XY coordinate location) in the raster grid and examining whether each hyperpoint is lower (i.e., obstructed) or higher (i.e., unobstrcuted) than the shadow casted by buildings for direct irradiance prediction. The latest raster-based approaches allow for capturing the urban fabric to predict irradiance on both roofs and facades from direct, diffuse and ground reflected irradiance. However, as calculation models used in the raster-based approaches are based on shadow cast or volume calculations, they are computationally expensive for large-scale irradiance predictions in urban areas.

Vector-based approaches use 3D shape files to represent the urban fabric, which can be created from GIS data or manually through drawing tools (e.g. CAD). With the 3D urban fabric model, advanced daylighting simulation software, particularly RADIANCE, has been applied to compute city-wide solar irradiance predictions (Jakebiec and Reinhart, 2013). RADIANCE is based on sophisticated calculation algorithms (i.e., ray tracing and radiosity) required to trace rays of light backwards from each viewpoint to the sources in a brute force manner (Larson and Shakespeare, 2004). As they require a huge amount of sampling rays and points for simulation, they do not effectively scale up to urban scale applications due to unnecessarily expensive computational cost. In order to reduce the computational cost associated with the complicated methods, Robinson and Stone (2004) developed the Simplified Radiosity Algorithm (SRA) by making incremental simplifications to the radiosity algorithm. However, existing vector-based calculation methods are yet not well suited for urban-scale applications as incremental changes are not sufficiently enough to relieve the expensive computational cost.

In terms of data collection and model construction, latest raster-based approaches rely on LiDAR technology that is usually expensive and not easily accessible. Furthermore, processing data from LiDAR is an intensive process dependent on highly specialised skills, makes it difficult to be part of common practices in the building domain. As the GIS data is available only for existing urban infrastructure, raster-based approaches require manual creation of an urban model to assess planned development in urban areas or different planning guidelines with their impact on irradiance distribution. On the other hand, vector-based approaches well align with current design practices as most drawing software packages are based on vector-based approaches. Hence, they enable utilising 3D models already created as part of a design process for design analysis. For existing urban areas, creating a 3D urban model is labour consuming. This problem can be overcome in the near future as there is the growing database of 3D urban models: for instance, urban 3D models for every city in the UK are available in EDiNA (EDiNA, 2017).

Additionally, the existing methods are developed to generate accurate predictions provided a model with correctly assigned thermal properties (mainly reflectance rate). In reality, however, building geometries are often simplified to rectangular boxes and the same set of thermal properties that represent the average is assigned to all buildings for urban-scale analyses to reduce the labour work assigning individual properties for each surface. Hence, there is the urgent need to tailor and simplify the irradiance prediction model according to the average thermal properties with changes for urban-scale applications.

The paper proposes a simplified vector-based method tailored for predicting solar potentials of urban surfaces in urban environments. First, the paper reviews three major components in the existing vector-based methods in detail and discusses their key limitations in the context of urban applications. Then, the paper presents a new method tailored for target applications. The performance of the proposed method is compared against the advanced simulation software, RADIANCE, through three cases with varying urban densities.

Existing vector-based methods

Predicting irradiation in urban contexts require three major components: (1) sky model based on sky discretized method that predicts varied brightness over the sky dome; (2) obstruction algorithm that identify the visible part of the sky and the sun from any viewpoint; (3) reflection algorithm that computes the amount of irradiance reflected by the urban fabric.

Sky discretization

Diffuse solar radiance across the sky dome is not uniformly distributed. The brightness of a specific point on the sky dome in a sunny day depends on its relative position to the sun curriculum, the sky zenith. In order to capture the non-uniform distribution, sky discretization techniques have been developed, and the Tregenza method (Tregenza et al., 1993) is the most widely used method in the existing daylighting simulation software including RADIANCE. The method divides the sky vault into 145 similar-sized patches, and the centre point of the patch is used to calculate a diffuse radiation value for the entire patch area as illustrated in Figure 1. For cases where higher accuracy is needed, Reinhart et al. (2000) proposed a method that divides the sky dome into 540 smaller-sized patches on the basis of the same discretization principle. Except the number of patches, these approaches create fixed shapes of patches with similar sizes covering the sky dome, and this uniform discretisation approach generates a large number of sky patches that may not be necessary to capture real urban obstruction situations with accuracy.

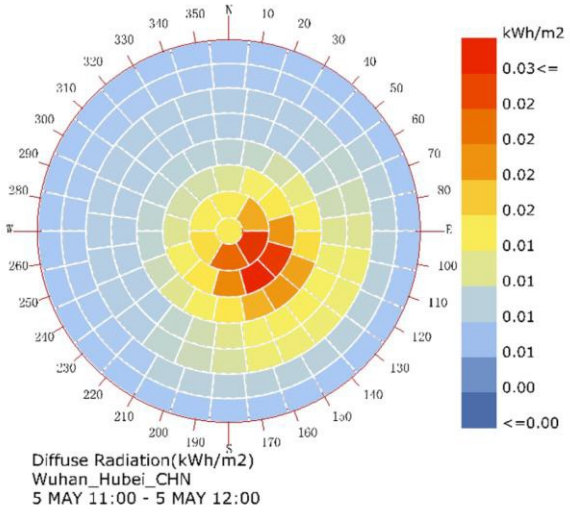

Figure 1 Diffuse radiance distribution using Tregenza independent discretization method.

In reality, most buildings are a solid mass starting from the ground level, with varying heights. Hence, it is unlikely to have part of buildings blocking only some patches in the middle of the sky (the left side of Figure 2) as buildings obstruct the sky from the ground level (the right side of Figure 2). Hence, the existing methods based on the uniform discretisation do not efficiently represent the non-uniform diffuse solar radiation of the unobstructed sky dome with the minimal number of sky patches required for reliable predictions. In fact, the number of sky patches used in the simulation significantly impacts the computational efficiency as it is required to check whether every testing point has an unobstructed view to each sky patch of the dome. Alternatively, if the highest point blocked by buildings, projected on the sky, is calculated first, all sky patches vertically below the highest point are completely invisible and,

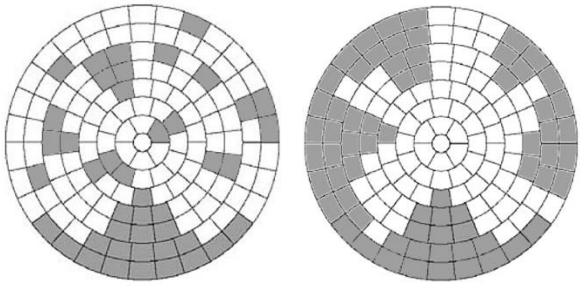

Figure 2 Unrealistic obstruction in urban environments (left); realistic obstruction in urban e

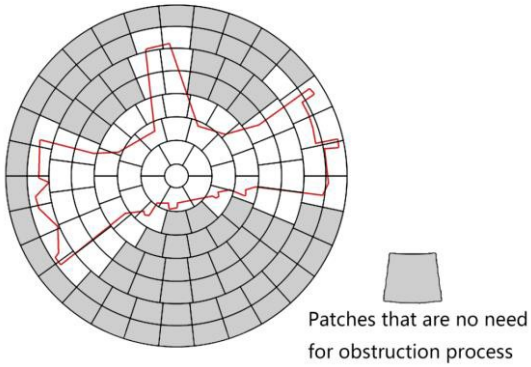

Figure 3 Lower sky patches do not need to be processed for obstruction

therefore, there is no need to divide the obstructed sky dome into small-sized patches. As illustrated in Figure 3, the existing discretisation methods create a substantial number of unnecessary sky patches, which significantly increase the computational inefficiency.

Obstruction detection algorithm

Ray tracing and SRA have been commonly used to detect urban surfaces that obstruct part of the sky dome. Both the methods rely on the ray intersection algorithm (Mitchell et al., 1990). In analytic geometry, the ray intersection algorithm detects the intersection between a line drawn from a testing point to a target area and a plane (i.e., potential obstruction) by creating raying from a testing point to all directions and computing the empty set (i.e., indicating no intersection), a point (i.e., where intersection happens), or a line (i.e., ray and plane are parallel without intersection). This computational technique has been widely used in computer graphics, motion planning, and collision detection. Using these methods for urban-scale applications requires intensive computational burdens as urban areas includes a large number of surfaces. The existing methods require creating a number of rays from every testing point of urban surfaces to each sky patch of the dome, and intersection calculations are carried out for each ray given a pair of a testing point and an urban surface. Figure 4 illustrates the basic concept of the methods. This approach demands a huge amount of iterations in

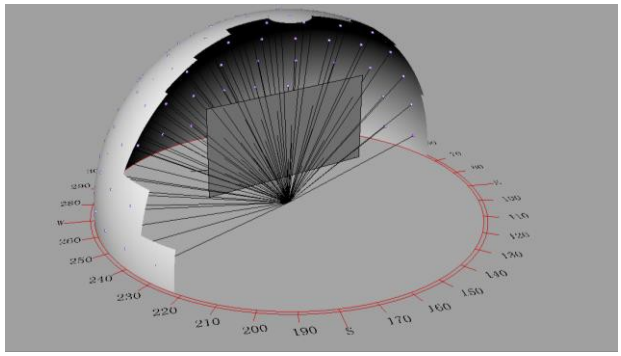

Figure 4 Existing method: Trace back rays to every sky sampling point for each surface to solve intersection formulas.

the intersection calculation, which is equivalent to the product of the number of testing points, the number of urban surfaces, and the number of sky patches. This computational algorithm is extremely expensive for large-scale problems and takes up to 95% of the total simulation time (Amanatides et al,. 1987).

Reflection algorithm

In urban areas, building surfaces, vegetation, and roads reflect both direct beam and diffuse radiations. Ray tracing and radiosity methods are used to trace light rays bounced between objects until the expected convergence is achieved. For instance, RADIANCE is based on the ray tracing method and iteratively calculates the trace of rays reflected by surfaces for every ray from the sky and the sun. In order to reduce the complexity in the reflection calculation for the urban-scale applications, SRA developed by Robinson and Stone (2004) assumes that surfaces are Lambertian (i.e., fully diffused). This assumption allows for substantially reducing a number of iterations in the calculation process, as there is no need to separately calculate beam reflection and diffuse reflection. Nevertheless, this simplified method is still computational demanding as it iteratively detects where reflection takes place and computes a series of diffused rays reflected by many surfaces in urban environments.

In addition the computational expense, all detail information about surface thermal properties is often unavailable and it is economically infeasible to obtain such detailed information about individual surfaces required for accurately calculating reflected irradiance on individual surfaces. Hence, urban-scale applications often assume surface thermal properties identically applied to all surfaces with the same type (Juan et al., 2013). Hence, the relevance of using high-fidelity methods should be carefully investigated under real urban applications where insufficient data about individual surface thermal properties are unavailable.

Proposed method

Sky discretization

As an alternative to the uniform discretization method, we propose a two-segment discretization method tailored for irradiance prediction in urban environments. As buildings block the sky from the horizontal level up to a certain level depending on their heights, the proposed method divides one sky strip into two segments: one segment blocked by buildings (from the ground to the highest point of the buildings projected to the sky dome) and the other segment with an unobstructed view to the sky (from the highest point to the sky zenith) as shown in Figure 5. In the proposed method, the sky dome is divided into N number of strips, referred to as Sky Horizontal Subdivision (SHS). SHS can vary depending on the required prediction accuracy, which is tested through the case study in the latter section. In the proposed method, subdivided sky strips have the same azimuth range, $\Psi = 2\pi/N$, and the Sky View Factor (SVF) of the i[th] sky strip is defined in terms of the altitude of the highest blocked point from a testing point, , as below

$$SVFi = 1 - sin\,\xi i. \quad (1)$$

.

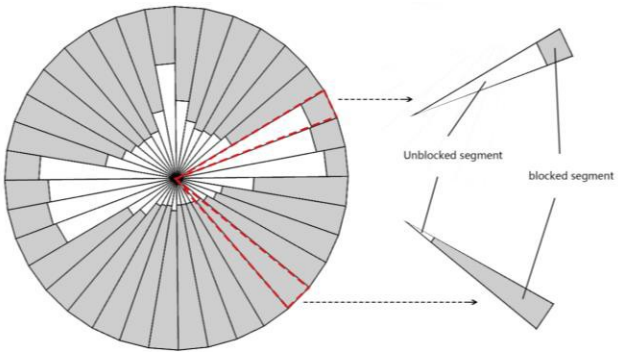

Figure 5 Illustration of a two-segment sky discretization method.

For dense urban areas where building heights within one sky strip vary dramatically, one may need to increase the SHS to correctly capture the obstructed skyline at the cost of high computational expense as the number of sky patches determines the number of calculation iterations. Instead of increasing the SHS, we introduce an additional step that calculates an average SVF for each sky strip with consideration of varying building heights within one sky strip. This step further subdivides each sky strip into K number of slices as shown in Figure 6; K is referred to as Strip Inside Subdivision (SIS).

In order to calculate the non-uniform irradiance received from the visible sky, each sky trip is assigned with M sampling points evenly spaced across the strip as illustrated in Figure 7; M is referred as Sky Radiance Sampling Subdivision (SRSS). However, only sampling points that fall within unblocked segments are selected for further calculations. In this way, the proposed method does not only allow for reducing the number of sky patches used for simulation but also gives a flexibility to users to make incremental adjustments as opposed to the Tregenza and similar approaches that provide the fixed discretization strategy.

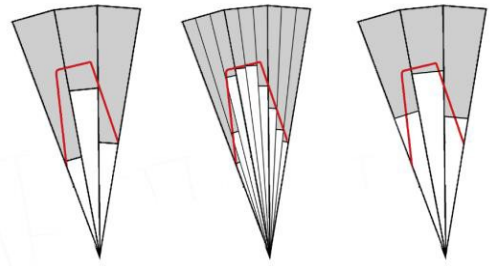

Figure 6 Illustration of using SIS for calculation of average sky view factors.

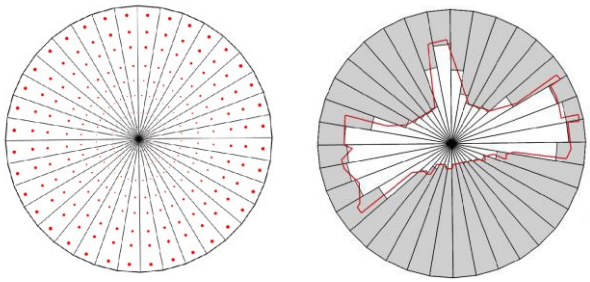

Figure 7 Illustration of radiance sampling points of the proposed method within the two-segment method.

Obstruction detection algorithm

As an alternative to tracing rays to intersect with all surfaces constituting the urban fabric, we propose a computationally efficient technique that identifies and computes the highest blocked point of buildings from a viewpoint. Figure 8 illustrates the basic concept behind the algorithm. First, building edge lines are divided by Building Edge Subdivision (BES) that indicates the distance between the subdivisions in the unit of meters; for example, if BES is set at three, there will be a sampling point every three meters along the building edge lines. Given a set of computed angles associated with all sampling points, the algorithm selects the highest angle from one viewpoint to each sky strip in order to discretize each sliced sky strip into unblocked and blocked segments.

The proposed method requires a much reduced number of calculation iterations than the existing methods as the total number of iterative calculations is the product of the number of viewpoints and sampling points. Furthermore, the proposed method allows users to flexibly set up (adjust) subdivision resolutions.

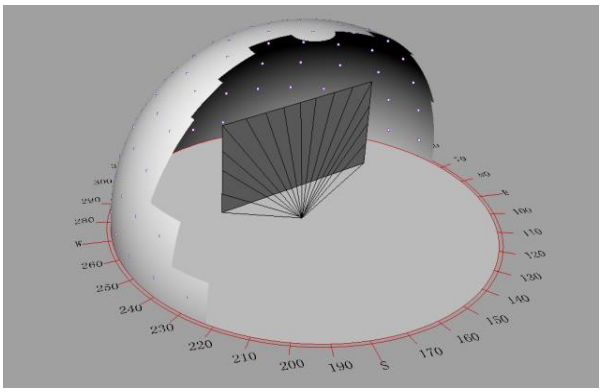

Figure 8 Illustration of calculating the highest obstruction point for each sky trip.

Reflection algorithm

Following the previous study by Robinson and Stone (2004), we assume that all surfaces are Lambertian in order to reduce the complexity in the reflection calculation process. We made three more simplifications to make the method much more simplified. First, as buildings and the ground are major surfaces in urban environments we only consider building and ground reflection. Second, instead of using individual surface thermal properties, we use only two average solar reflectance values: one for all building surfaces and the other for ground surfaces. Third, only solar irradiance reflected in the first bounce is considered.

Similar to the way to calculate SVF, we introduce the concept of Building View Angle (BVA) and Ground View Angle (GVA) as illustrated in Figure 12. BVA and GVA are defined as the solid angle of visible building surfaces and ground surfaces from a viewpoint, respectively. In the ith sky strip, BVA and GVA are given as:

$$BVA = \frac{2\pi}{N}(\sin(\xi i) + |\sin(\beta)|) \quad (2)$$

$$GVA = \frac{2\pi}{N}|\sin(\beta i)|. \quad (3)$$

where N is SHS and in each sky trip, ξ_i and β_i are the altitude of the highest and lowest blocked points, respectively.

With BVAs and GVAs obtained, the proposed method calculates reflected irradiance through three steps. First, average reflectance vales, ρ_b for buildings and ρ_g for the ground, are estimated on the basis of general observation of a case study area. If additional information including measurements from the case study area is available, they will improve the accuracy of the average values and consequently the confidence level of predictions. Second, the average first-received irradiance R_b and R_g is calculated separately for building surfaces and ground surfaces. Then, the total first-bounce reflected irradiance from buildings $G_{building}$ and that from ground G_{ground} on a viewpoint is given as:

$$G_{building} = R_b * BVA * \cos(\sigma_b) \quad (4)$$

$$G_{ground} = R_g * GVA * \cos(\sigma_g) \quad (5)$$

Where σ_b and σ_g is the angle between the surface normal and the line that connects the view point to the centre point of building view and ground view accordingly in that sky strip.

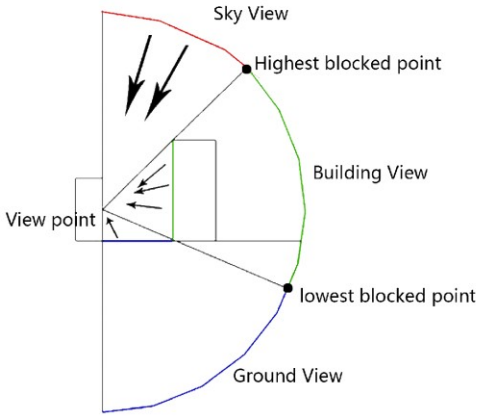

Figure 9 Illustration of the concept using three view factors

Since the proposed method considers only one bounce of reflection, this assumption may likely underestimate the reflection prediction. Reflected irradiance is commonly considered as much less than the first received irradiance from daylight. Indeed, several research studies (Redweik, et al., 2013;Lindberg, et al., 2015) also used one-time reflection approach for ground reflection and did not consider reflection between buildings. As the effect of this simplification has not been investigated yet, we will investigate the effect of the simplification on the total irradiance predication through a case study in the future.

Other model components

The proposed model uses the Perez All-Weather model for predicting a diffuse radiance output for each sky sampling point. The Perez All-Weather model has been validated against measurements and popularly used in simulation studies (Diez-Mediavilla, et al., 2005). In the model, the radiance of each sky point is given as R= I_Z*L_v* I_r, where I_z is zenith luminance which can be either provided by the latest weather files such as TMY3 or generated by the Perez zenith luminance model, L_v is the relative luminance factor defined as the ratio of the luminance of a sampling point to the luminance of sky zenith, I_r is the relative factor to convert luminance to radiance. Detailed description about the model is provided in Perez's work (Perez et al., 1990, Perez et al., 1993).

With the radiance given by the Perez model, the diffuse irradiance received on the target viewpoint from each of the visible sky sampling point is defined as:

$$G_{diff} = R\cos(\alpha_{diffuse})\,\Phi \quad (6)$$

Where R is radiance of a sky patch calculated by the Perez model, Φ is the solid angle of the visible sky patch. $\alpha_{diffuse}$ is the incident angle on the surface at the viewpoint from the sky patch.

As direct irradiance (i.e., beam daylight) only comes from the position of the Sun. we only need to check whether the sun can be seen from the viewpoint. If the solar altitude $\xi_{sun} > \xi_i$, where ξ_i is the altitude of highest blocked point in that sky strip mentioned earlier, then the Sun is visible from the view point in that sky trip, otherwise not. If the Sun is visible, direct irradiance is given as:

$$G_{direct} = DNI \times cos(\alpha_{direct}) \quad (7)$$

Where DNI is the direct normal irradiance derived from weather data, α_{direct} is the incident angle between the direct beam and the surface at the viewpoint.

Case study

The proposed method is implemented in Python, particularly using the tool package called as Numpy. Numpy provides useful techniques such as broadcasting and array vectorization to avoid and replace the low-efficient loops iteration calculation, which facilitates achieving the computational efficiency.

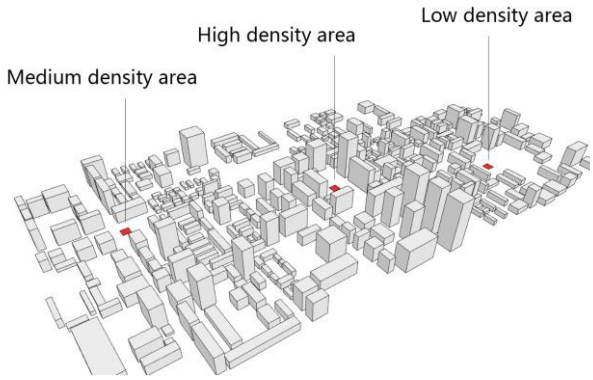

Figure 10 Illustration of the urban geometry and selected areas for testing

The performance of the method is tested by three cases with varying urban densities. We created an urban model a 0.72 km^2 city area (1.2 km*0.6 km) located in Hankou district in Wuhan, China. Urban geometry in the model only includes buildings and ground surfaces. In the studied area, we locate a testing surface in three areas with different densities, ranging from relatively high density to low density, as displayed in Figure 10. The total irradiance for the flat plane of 20 m*20 m is obtained by calculating the irradiance of 36 testing points spaced by a 3 m-by-3 m grid. Building envelope and ground reflectance values are assumed to be 0.2 and 0.1, respectively. The CSWD (Chinese Standard Weather Data) created by the China Meteorological Bureau is used to provide hourly direct and diffuse radiation data and dew point temperature. Unlike the TMY3 weather file, the CSWD does not provide the zenith luminance data. Therefore, the Perez's zenith luminance model is used to generate zenith luminance outputs. Using a pre-process accumulated sky technique (Robinson and Stone 2004), the computational cost changes insignificantly from calculating one single day to an entire year. Thus we select March 1st as a simulation period as this day presents both direct and diffuse daylight with changes within a day while representing typical weather conditions.

Effect of control parameters

This section investigates the effect of the control parameters used in the analysis settings on both prediction accuracy and computational efficiency. The control parameters are Sky Horizontal Subdivision (SHS), Strip Inside Subdivision (SIS), Sky Radiance Sampling Subdivision (SRSS), and Building Edge Subdivision (BES). Table 1 shows the ranges of the control parameter values with their base values. We perform differential sensitivity analyses to examine the effect of individual control parameters by change one parameter value while keeping the rest parameters fixed at the base value. The resulting outcomes will help optimize the analysis settings in order to achieve a balance between prediction accuracy and computational efficiency.

Table 1: Value range for each parameter

Setting parameter	Range			base value
SHS	3	-	36	24
SIS	1	-	4	2
SRSS	3	-	18	9
BES	1	-	11	3

Fig.11-14 show irradiance predictions and associated computational costs with different parameter settings. Overall, SHS is the most dominant parameter that impacts the predication accuracy most in comparison to the other parameters. For SHS, incremental changes up to 18 significantly impacts the prediction results, especially for the high density scenario. Further increase in SHS does not impact the prediction accuracy although it linearly increases the computational time. SIS also shows the similar trend, and the prediction accuracy noticeably improves until SIS value increases up to 2. The SRSS setting, however, does not show a substantial impact on the prediction accuracy nor does it noticeably increase the computational cost. Since the time cost does not change much with the increase of SHS, we selected 9 as the setting for further analyses. Changes in the BES setting also do not change the prediction accuracy. As using the fine resolution of 1 m for BES exponentially increases the computational load, we selected 3 for the BES setting. However, the effect of BES may be influenced by the case study area used for this analysis. In the case study, the buildings are quite massive and are not located closely nearby, which means a relatively low resolution of BES could still provide enough accuracy. In other urban areas where buildings are smaller and denser, the effect of

BES would be more dominant and need to be carefully considered. In addition, the results suggest that crude analysis settings provide prediction outcomes as accurately as more refined analysis settings for the low-density case whereas the analysis settings need to be carefully designed for urban cases with higher densities.

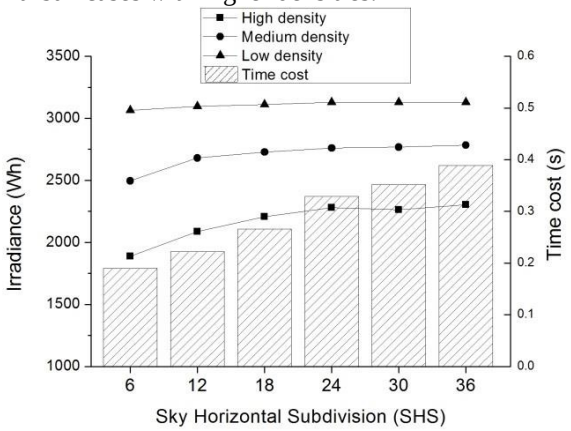

Figure 11 Impacts on results from SHS

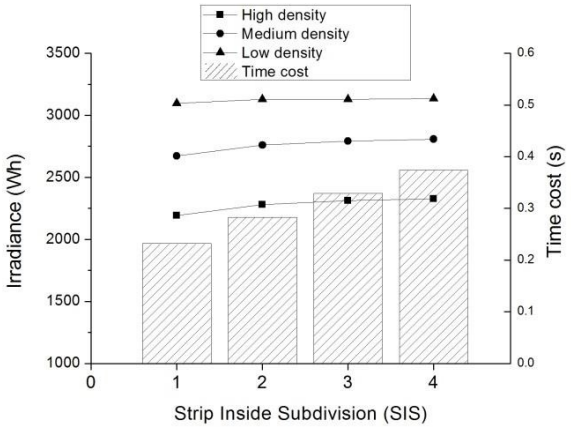

Figure 12 Impacts on results from SIS

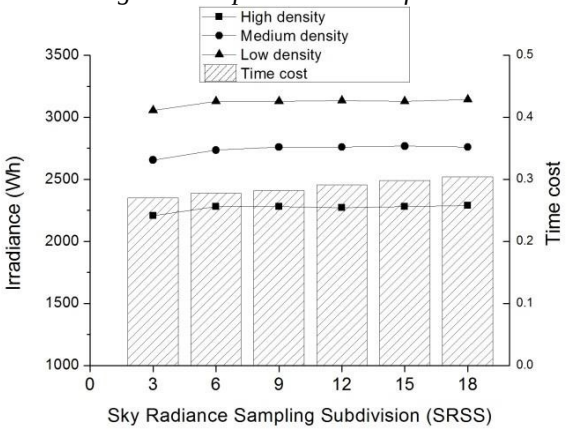

Figure 13 Impacts on results from SRSS

Comparison against RADIANCE

RADIANCE is regarded as one of the most advanced simulation tools designed for lighting simulation and uses the sophisticated ray tracing algorithm for calculation of obstruction and reflection. In order to validate the proposed model, we compare

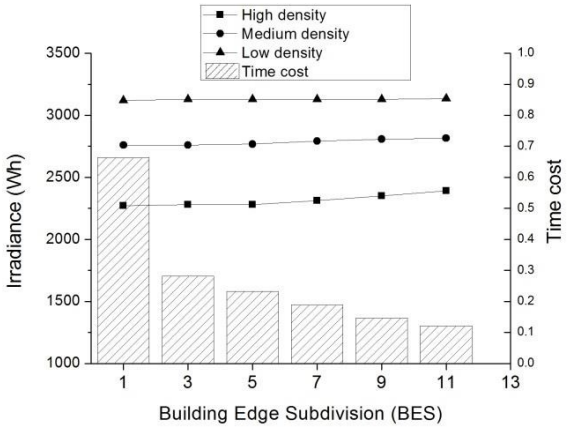

Figure 14 Impacts on results from BES

outcomes predicted by the proposed method with those by RADIANCE through the case study described above. We used the HoneyBee toolkit in Grasshopper that facilitates creating/managing a large-scale urban model and using RADIANCE to obtain simulation outputs. We chose a medium level default setting provided by HoneyBee; in this setting, the number of reflection is set at 3.

A plane at different tilted angles shown in Figure 15 is used to predict accumulated irradiance during the test day (8:00 AM to 4:00 PM) under the three urban areas. Tables 2-4 show accumulated irradiance predictions by the proposed method in comparison to those by RADIANCE.

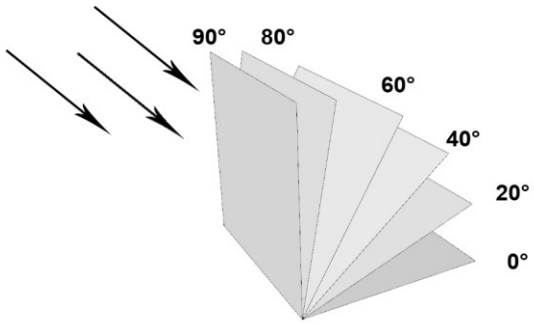

Figure 15 Planes at different tilt angles

Table 2: Comparison results (High density area)

Plane tilt	Radiance (Wh)	Proposed method (Wh)	Difference
0	2176	2295	5.47%
20	2422	2593	7.06%
40	2437	2621	7.55%
60	2189	2325	6.21%
80	1693	1702	0.53%
90	1392	1261	-9.41%

Table 3: Comparison results (Medium density area)

Plane tilt	Radiance (Wh)	Proposed method (Wh)	Difference
0	2711	2795	3.10%
20	2986	3132	4.89%
40	2979	3086	3.59%
60	2657	2712	2.07%
80	2082	1971	-5.33%
90	1715	1588	-7.41%

Table 4: Comparison results (Low density area)

Plane tilt	Radiance (Wh)	Proposed method (Wh)	Difference
0	2941	3133	6.53%
20	3267	3372	3.21%
40	3353	3412	1.76%
60	3079	3125	1.49%
80	2463	2434	-1.18%
90	2142	2081	-2.85%

Overall, the proposed method yielded irradiance predictions that are in good agreement with RADIANCE. For the low density case, the proposed method results in predictions within an average difference of less than 3% in comparison to RADIANCE. However, prediction differences rise up to 7.4% for the medium density area and up to 9.4% for the high density area. The larger prediction differences for dense urban areas suggest that the proposed method is less able to accurately capture a more complex urban geometry in higher density areas. In addition, the proposed method overestimates irradiance on the horizontal planes while underestimating that on the verticalsurfaces. Underestimated irradiance for vertical surfaces can be due to the simplified reflection model in which only the first-bounce reflection is considered. As the result, the simplified model may miss out some of the reflected irradiance, particularly on vertical surfaces (mostly walls) where a considerable amount of reflected daylight may be received from both the ground and surrounding buildings.

In addition to the prediction accuracy for the testing plane, we evaluate the accuracy of predictions for large-scale design applications where a total or average amount of solar energy obtained at the district or neighbourhood scale is the core interest. For the large-scale analysis, we compute irradiance predictions for every building surface of the entire area; the entire area includes 337 individual buildings. Table 5 compares the total irradiance on the entire set of building surfaces predicted by the two methods. The results predicted by the proposed method closely matched those by RADIANCE. More importantly, the proposed method reduces the computational time significantly. This comparison indicates the large potential of the simplified method for large-scale urban applications.

Table 5 Total irradiance of a large-scale interest

	RADIANCE	Proposed method	Difference
Irradiance	1,574,473 (kWh)	1,515,531 (kWh)	3.74%
Time cost	21643s	266 s	

Conclusion

This paper presented a simplified vector-based method that allows for efficiently predicting solar potentials in urban areas with proper consideration of the urban context. The paper described a simplified yet physics-based method for solar irradiance prediction in urban areas. Comparison of the new method against the existing advanced method demonstrated that the new method significantly improves the computational efficiency while providing reasonably accurate predictions to support large-scale solar analysis.

As reflecting the urban context, the proposed sky discretization method reduces the number of sky patches that correctly capture the non-uniform diffuse irradiance. As the result, the method significantly improves the computational efficiency as shown in the case study. The angle detection method together with the simplified reflection algorithm also substantially contributes to reducing the calculation load. However, the new method tends to underestimate reflected irradiance predictions for walls in highly dense areas. Further work will be needed to enhance the reflection model.

The new method also provides users with flexibly setting control parameters related to the analysis setup: Sky Horizontal Subdivision (SHS), Strip Inside Subdivision (SIS), Sky Radiance Sampling Subdivision (SRSS), and Building Edge Subdivision (BES). SHS is found to be the most dominant parameter that impacts the prediction accuracy. Changes in the setting do not impact the prediction accuracy noticeably for the low-density case area whereas they play a substantial impact for the dense urban areas. Further work is needed to provide guidance on optimal control settings in relation to the characteristics of urban contexts.

Acknowledgement

The work presented here was supported by Cambridge-CSC Scholarship, the National Nature Science Fund of China (Project No. 51678261), and Urban Science and Technology Program of Wuhan (Project No. 201726).

Reference

Amanatides J, Woo A (1987). A fast voxel traversal algorithm for ray tracing. *Eurographics 87(3)*, 10.

Compagnon R (2004). Solar and daylight availability in the urban fabric. *Energy and buildings* 36(4), 321-328.

Diez-Mediavilla M, De A, Bilbao J. (2005). Measurement and comparison of diffuse solar irradiance models on inclined surfaces in Valladolid (Spain). *Energy Conversion and Management 46(13)*, 2075-2092.

EDiNA (2017). http://digimap.edina.ac.uk/.

Fu P, Rich M (2002). A geometric solar radiation model with applications in agriculture and forestry. *Comput. Electron. Agric* 37,25-35.

Hofierka J, Suri M (2002). The solar radiation model for Open source GIS:implementation and applications. *Proceedings of the Open source GIS - GRASS Users Conference.*

Hofierka J, Kanuk J (2009). Assessment of photovoltaic potential in urban areas using open-source solar radiation tools. *Renewable Energy 34*, 2206 – 2214.

Jakubiec J, Reinhart C (2013). A method for predicting city-wide electricity gains from photovoltaic panels based on LiDAR and GIS data combined with hourly Daysim simulations. *Solar Energy 93*,127-143.

Kanters J, Wall M (2016). A planning process map for solar buildings in urban environments. *Renewable and Sustainable Energy Reviews* 57, 173-185.

Lindberg F, Jonsson P, Honjo T, Wästberg D. (2015). Solar energy on building envelopes – 3D modelling in a 2D environment, *Solar Energy* 115, 369-378

Lauson G, Shakespeare R (2004). Rendering with RADIANCE: the art and science of lighting visualization. *Booksurge Llc.*

Mitchell P (1990). Robust Ray intersection with interval arithmetic, *Proceedings of Graphics Interface 90*, 68-74.

Perez R, Ineichen P, Seals R, et al (1990). Modeling daylight availability and irradiance components from direct and global irradiance. *Solar energy 44(5)*, 271-289.

Perez R, Seals R, Michalsky J (1993). All-weather model for sky luminance distribution—preliminary configuration and validation. *Solar energy 50(3)*, 235-245.

Robinson D, Stone A (2004). Solar radiation modelling in the urban context. *Solar energy 77(3)*, 295-309.

Robinson D, Stone A (2004). Irradiation modelling made simple: the cumulative sky approach and its applications. *PLEA Conference*, 19-22.

Reinhart C, Herkel S (2000). The simulation of annual daylight illuminance distributions — a state-of-the-art comparison of six RADIANCE-based methods. *Energy and Buildings 32(2)*, 167-187.

Ratti C, Richens P (2004). Raster analysis of urban form. *Environment and Planning B: Planning and Design 31(2)*, 297-309.

Redweik P, Catita C, Brito M (2013). Solar energy potential on roofs and facades in an urban landscape. *Solar Energy* 97, 332-341.

Roudsari S, Pak M, Smith A (2013). Ladybug: a parametric environmental plugin for grasshopper to help designers create an environmentally-conscious design. *In: Proceedings of the 13th International IBPSA Conference*, 3128-3135.

Sarralde J, Quinn D, Wiesmann D, Steemers K (2015). Solar energy and urban morphology: Scenarios for increasing the renewable energy potential of neighbourhoods in London. *Renewable Energy 73*, 10-17

Tregenza P, Sharples S (1993). Daylighting algorithms. *ETSU S 1350, U.K. Department of TRADE and Industry on Behalf of the Energy Technology Support Unit*, 43.

Vangimalla R, Olbina J, Issa R, et al (2011). Validation of Autodesk Ecotect™ accuracy for thermal and daylighting simulations. *Proceedings: Simulation Conference (WSC)*, 3383-3394.

Zomer C, Rüther R (2017). Simplified method for shading-loss analysis in BIPV systems–part 1: Theoretical study. *Energy and Buildings 141*, 69-82.

Nomenclature

BVA	Building View Angle
DNI	Direct normal irradiance
$G_{building}$	First-bounce reflected irradiance from buildings

G_{diff}	Diffuse irradiance receive by each of the visible sky sampling point
G_{direct}	Direct irradiance
G_{around}	First-bounce reflected irradiance from ground
GVA	Ground View Angle
I_r	Relative factor to convert luminance to radiance
I_z	Zenith luminance
K	Strip Inside Subdivision
L_v	Relative luminance factor
M	Sky Radiance Sampling Subdivision
N	Sky Horizontal Subdivision
R	The radiance of each sky point
R_b	Average first-received irradiance for building surfaces
R_g	Average first-received irradiance for ground surfaces
SVF	Sky View Factor
α_{direct}	The angle from the view point to the Sun.
β	Altitude of the lowest blocked points
ξ_i	Altitude of the highest blocked point in the i^{th} sky strip
ξ_{sun}	Solar altitude
ρ_b	Average reflectance rate of buildings
ρ_g	Average reflectance rate of ground
σ_b	The angle between the surface normal of the viewpoint to the center point of building view
σ_g	The angle between the surface normal of the viewpoint to the center point of ground view
φ	Solid angle of the visible sky patch
ψ	Azimuth range